JRMP Journal of Radiopharmaceuticals and Molecular Probes Vol. 7, No. 1, 2021
J Radiopharm Mol Probes 2021;7(1):56-65
ISSN 2384-1583(Print) / ISSN 2508-3848(Online)

PROTOCOL

https://doi.org/10.22643/JRMP.2021.7.1.56

Synthesis of dimeric fluorescent TSPO ligand for detection of glioma

Tien Tan Bui[1,2], Hee-Kwon Kim[1,2*]

[1]Department of Nuclear Medicine, Molecular Imaging & Therapeutic Medicine Research Center, Jeonbuk National University Medical School and Hospital, Jeonju, Korea
[2]Research Institute of Clinical Medicine of Jeonbuk National University-Biomedical Research Institute of Jeonbuk National University Hospital, Jeonju, Korea

ABSTRACT

TSPO, an 18-kDa translocator protein, is a peripheral-type benzodiazepine receptor that has been associated to a variety of biological activities such as apoptosis, steroidogenesis, and cell proliferation. Because TSPO overexpression has been found in various forms of cancer, it has recently become one of the most appealing biological targets for cancer therapies and detection. In order to create new optical imaging agents for improved diagnostics, we synthesized a novel dimeric fluorescent TSPO ligand based on PRB28 structure and SCy5.5. Following the preparation of the novel TSPO ligand, *in vivo* and *ex vivo* imaging tests were performed to examine the tumor uptake characteristics of the fluorescent TSPO ligand in a glioma animal model, and it was found that novel TSPO ligand was accumulated in glioma. These results suggested that novel dimeric fluorescent TSPO ligand will be applied to detect glioma.

Key Word: Translocator protein, Glioma, Molecular imaging, NIR fluorescent probe

Introduction

The translocator protein (18 kDa) (TSPO), which was previously categorized as a kind of peripheral benzodiazepine receptor, is a five transmembrane sphere protein found primarily on the outer surface of mitochondrial membranes [1, 2]. TSPO is also distributed predominantly in steroid-producing organs, including the brain [3–7]. From hydropathy characterization of the 169-amino-acid TSPO, the structure of TSPO was experimentally confirmed as five transmembrane helices [8].

Moreover, TSPO has been associated with a variety of fundamental biological functions, including steroidogenesis, heme biosynthesis, oxidative stress, cell proliferation and differentiation, cell cycle, mitochondrial respiration, mitochondrial membrane potential, and so on [1]. Aberrant TSPO expression was connected with multiple forms of cancer including breast, colon, prostate, and ovarian tumors, as well as astrocytoma, hepatocellular, and endometrial carcinomas [9,10]. Furthermore, because TSPO overexpression is associated with microglial activation in the brain, particularly in the central nervous system, and TSPO levels are lowest in resting microglia, TSPO may be a feasible biomarker for inflammatory neurodegenerative disor-

Received: June 14, 2021 / **Revised:** June 26, 2021 / **Accepted:** June 28, 2021

Corresponding Author: Hee-Kwon Kim, Department of Nuclear Medicine, Jeonbuk National University Medical School and Hospital, Jeonju, Jeonbuk 54907, Republic of Korea, Tel: +82 63 250 2768, Fax: +82 63 255 1172, E-Mail address: hkkim717@jbnu.ac.kr

ders such as Alzheimer's disease, Parkinson's disease, Huntington's disease, and multiple sclerosis [11].

Many clinical studies have used TSPO ligands. The first synthesized TSPO ligand was built on the isoquinoline carboxamide structure (PK11195), which specifically binds to the peripheral benzodiazepine receptor, classified as TSPO ligand with high affinity [12]. [^{11}C]-PK11195, a PET tracer of this TSPO ligand, has been used to detect brain inflammation in patients with neurodegenerative disorders such as Huntington's disease and Parkinson's disease [13]. With the tremendous achievements in this area, various TSPO ligands have been discovered, including phenoxyaryl acetamide (PBR28 and DAA1106), imidazopyridin-acetamide and its bioisosteric structures (CB148, DPA-713, and DPA-714), and indoleacetamides (SSR180575) [14].

Optical imaging is defined as a concept of non-invasive molecular imaging that utilizes simple and low-cost equipment, making it more reasonable and controllable for clinical imaging and preclinical research [15]. Furthermore, optical tracers could be stored, supplied, and used, with the added benefit of being mass-produced on a large scale [16]. One may also use several probes that emit a wide range of colors and simultaneously calculate the signals from different channels, allowing for the examination of various molecular properties at the same time [17, 18].

Near-infrared (NIR) fluorophores have recently emerged as new fluorescent agents, with benefits such as low background fluorescence signals and good penetration in deep tissues [19-21]. Many NIR fluorescence probes have been produced for a variety of applications, based on a wide range of materials such as small organic molecules, inorganic materials, or composites of organic and inorganic materials [22-24]. Small organic compounds, in particular, have been frequently employed due to their small size, flexibility in design, and biocompatibility [25, 26].

Gliomas are tumors that arise from glial cells and are the most common kind of cancer in the brain, particularly in the central nervous system (CNS). Glioblastoma multiforme (GBM) is the most lethal kind of glioma tumor, with a prognosis of just 1-2 years of survival dependent on the stage of isocitrate dehydrogenase (IDH) [27]. Glioblastomas have various features that contribute to their malignancy, including a rapid pace of development, extensive vascularization, and highly penetrative features. Therefore, molecular imaging, also known as non-invasive methods, such as X-ray computed tomography (CT), magnetic resonance imaging (MRI), positron emission tomography (PET), and others, has been developed over years in clinical investigations for the diagnosis of glioma [28].

Optical imaging probes based on TSPO ligands have now been used for the diagnosis of a range of diseases. For example, Kozikowski *et al.* [29] synthesized a TSPO optical probe using 4-chloro-7-nitrobenzofurazan (NBD chloride) and used it to visualize C6 rat glioma cells and MA-10 Leydig. Because a wide range of effective TSPO ligands have been discovered in recent years, the formation of novel fluorescence probes based on novel TSPO ligand moiety with high affinity to TSPO is a significant and important study. Particularly, PBR28 ligands containing moieties *N*-(2-hydroxybenzyl)-*N*-(4-phenoxypyridin-3-yl)acetamide have demonstrated substantial benefits in terms of selective target of TSPO, such as high affinity for nano-molar binding to TSPO and considerably improved signal-to-background noise ratio in several studies [30-32]. Herein, we describe protocol for the synthesis and evaluation of a new dimeric fluorescent TSPO ligand to examine its potential imaging abilities in a glioma cancer model (Scheme 1 and Scheme 2).

Materials

All reagents and solvents used for reactions were

Scheme 1. Synthetic procedures for preparation of *N*-(2-hydroxybenzyl)-*N*-(4-phenoxypyridin-3-yl)acetamide with PEG-NH_2

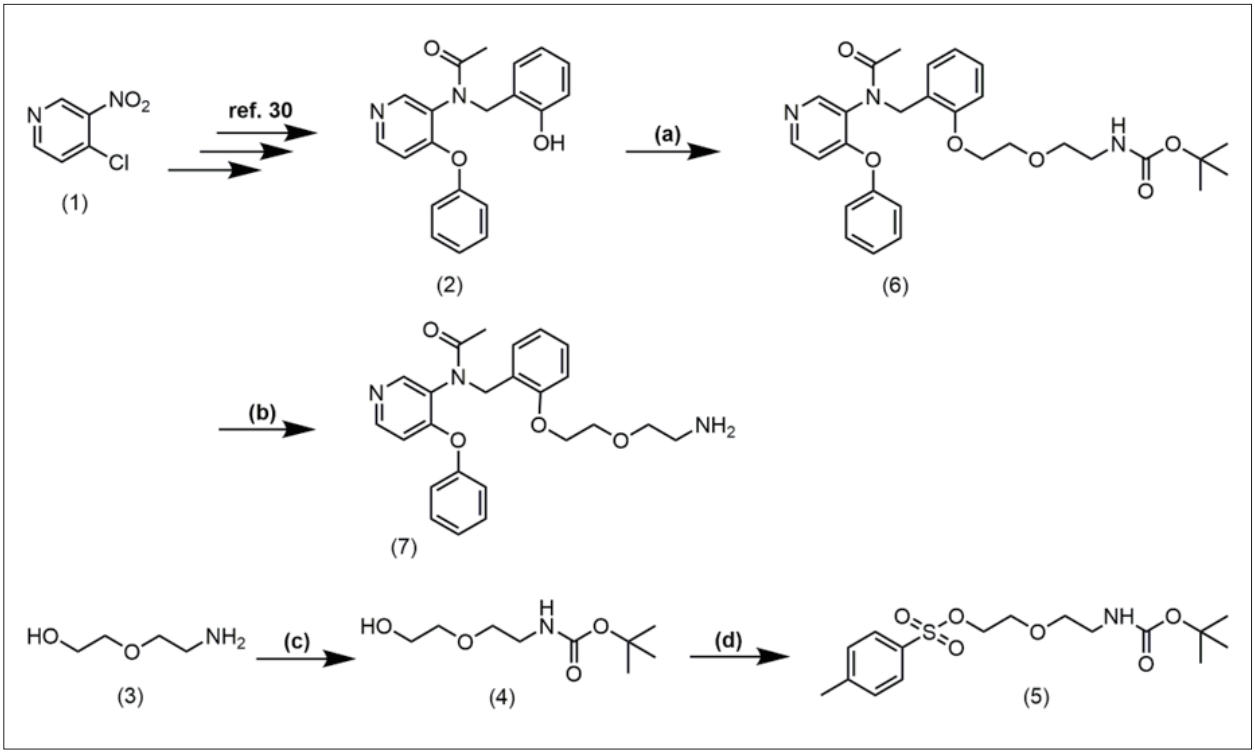

Reaction condition: (a) compound 5, K_2CO_3, acetonitrile, 80 °C, 19 h; (b) TFA, CH_2Cl_2, r.t., 3 h; (c) Boc_2O, THF, r.t., 1 h; (d) TsCl, aq. NaOH, H_2O/THF, r.t., overnight.

commercially available and used without any purification. Solvents for extraction and chromatography were reagent grade and used as received. Thin-layer chromatography as aluminum sheets coated with silica gel 60 F_{254} (Merck, Germany) were used to monitor the progress of these reactions. The products were detected by UV light (254nm) exposure or $KMnO_4$ stain. Flash column chromatography was performed using Merck silicagel 60 (0.040-0.063 mm) and eluted with proper mixture of solvents. Melting points of products were determined by a Stuart SMP10 melting point Apparatus (Cole-Parmer Ltd., UK). Nuclear magnetic resonance spectra (^1H and ^{13}C) were recorded on a 400 MHz spectrometer (Bruker, US) at room temperature in deuterated solvents with tetramethylsilane (TMS) as an internal reference. The chemical shift values were reported in δ units (ppm) relative to residual chloroform or dimethyl sulfoxide (DMSO), and the coupling constants (*J*) were quoted in hertz (Hz). High-resolution mass spectrometry was carried out by Mass Spectrometry Service of Jeonbuk National University and Korea Basic Science Institute.

Procotol

1. Synthesis of *N*-(2-hydroxybenzyl)-*N*-(4-phenoxypyridin-3-yl)acetamide (2)

The synthesis of the core TSPO structure (compound 2) was performed using 4-chloro-3-nitropyridine as starting material according to previously reported method [33].

2. Synthesis of tert-butyl(2-(2-(2-((*N*-(4-phenoxypyridin-3-yl)acetamido)methyl)phenoxy)ethoxy)ethyl)carbamate (6)

2.1) Compound **5** (3.00 g, 8.97 mmol) in anhydrous acetonitrile (10 mL) was added to a mixture of 2-(2-((tert-butoxycarbonyl)amino)ethoxy)ethyl 4-methylbenzenesulfonate (compound **3**) (3.91 g, 10.76 mmol) and K_2CO_3 (4.95 g, 35.89 mmol) in anhydrous acetonitrile (20 mL) at room temperature.

2.2) The mixture was heated to 80 °C and stirred for 19 h. The reaction mixture was quenched with H_2O (20 mL) and extracted with ethyl acetate (20 mL×2).

2.3) The combined organic layer was dried over anhydrous Na_2SO_4, filtered, and concentrated under reduced pressure.

2.4) The crude product was purified by flash column chromatography using n-hexane/ethyl acetate (1:2 to 1:4) as the eluent on silica gel to yield compound **6**.

3. Synthesis of *N*-(2-(2-(2-aminoethoxy)ethoxy)benzyl)-*N*-(4-phenoxypyridin-3-yl)acetamide (7)

3.1) Compound **6** (4.00 g, 7.67 mmol) was added to the mixture of TFA/CH_2Cl_2 (1:1, v/v) (5 mL).

3.2) The reaction mixture was stirred at room temperature for 3 h.

3.3) The reaction mixture was quenched with saturated solution of $NaHCO_3$ (20 mL), extracted with dichloromethane (20 mL × 2), and washed with brine (20 mL).

3.4) The combined organic layer was dried over anhydrous Na_2SO_4, filtered, and concentrated under reduced pressure to yield compound **7**.

4. Synthesis of tert-butyl (2-(2-hydroxyethoxy)ethyl)carbamate (4)

4.1) Di-tert-butyl dicarbonate (14.8 g, 68.48 mmol) was added to 2-(2-aminoethoxy)ethan-1-ol (6.00 g, 57.06 mmol) in anhydrous tetrahydrofuran (25 mL) at room temperature.

4.2) After being stirred at room temperature for 1 h, the reaction mixture was quenched with saturated $NaHCO_3$ (20 mL), extracted with ethyl acetate (20 mL), and washed with brine (20 mL).

4.3) The organic layer was dried over anhydrous Na_2SO_4, filtered, and concentrated under reduced pressure.

4.4) The residue was purified by flash column chromatography using n-hexane/ethyl acetate (2:1 to 1:1) as the eluent on silica gel to yield compound **4**.

5. Synthesis of 2-(2-((tert-butoxycarbonyl)amino)ethoxy)ethyl 4-methylbenzenesulfonate (5)

5.1) To compound **4** (10.65 g, 48.0 mmol) in tetrahydrofuran (10 mL), NaOH (3.84 g, 96.0 mmol) in water was added at room temperature.

5.2) The reaction mixture was cooled to 0 °C. p-Toluenesulfonyl chloride (10.98 g, 57.6 mmol) in tetrahydrofuran (20 mL) was added dropwise to the reaction mixture.

5.3) After being stirred at room temperature for overnight, the reaction mixture was concentrated under reduced pressure, then quenched with water (30 mL), and extracted with dichloromethane (30 mL × 2).

5.4) The combined organic layer was dried over anhydrous Na_2SO_4, filtered, and concentrated under reduced pressure.

5.5) The residue was purified by flash column chromatography using n-hexane/ethyl acetate (1:1) as the eluent on silica gel to yield compound **5**.

6. Synthesis of Benzyl (7,11-dioxo-1,17-bis(2-((N-(4-phenoxypyridin-3-yl)acetamido)methyl)phenoxy)-3,15-dioxa-6,12-diazaheptadecan-8-yl)carbamate (8)

6.1) *N*-Benzyloxycarbonyl-L-glutamic acid (0.31 g, 1.11 mmol), HOBt (0.449 g, 3.33 mmol), and 1-Ethyl-3-(3-dimethylaminopropyl)carbodiimide (EDC) (0.469 g, 3.33 mmol) was dissolved in anhydrous DMF (10 mL).

6.2) The mixture was stirred at room temperature for 15 minutes.

6.3) Compound **7** (1.400 g, 3.33 mmol) and Et_3N (5.55 mmol, 0.77 ml) in anhydrous DMF (5 mL) was added to the mixture.

6.4) After being stirred for 14 h at room temperature, the reaction mixture was quenched with water (40 mL) and extracted with ethyl acetate (40 mL × 3).

6.5) The combined organic layer was dried over anhydrous Na_2SO_4, filtered, and concentrated under reduced pressure.

6.6) The crude product was purified by flash column chromatography using dichloromethane/methanol (30:1 to 20:1) as the eluent on silica gel to yield compound **8**.

7. Synthesis of 2-amino-N^1,N^5-bis(2-(2-(2-((*N*-(4-phenoxypyridin-3-yl) acetamido)methyl) phenoxy)ethoxy)ethyl) pentanediamide (9)

7.1) To the mixture of compound **8** (0.400 g, 0.37 mmol) and thioanisole (0.230 g, 1.83 mmol), TFA (6 mL) were added at room temperature.

7.2) The reaction mixture was stirred at room temperature for 24 h.

7.3) The mixture was quenched with saturated sodium bicarbonate (10 mL) and extracted with dichloromethane (20 mL × 2).

7.4) The combined organic layer was concentrated under reduced pressure.

7.5) Dichloromethane (5 mL × 5) was added to crude product and concentrated under reduced pressure until thioanisole was fully removed.

7.6) The crude mixture contained compound **9** was used directly for next reaction without further purification.

8. Synthesis of Potassium3-(6-((7,11-dioxo-1,17-bis(2-((*N*-(4-phenoxypyridin-3-yl) acetamido)methyl)phenoxy)-3,15-dioxa-6,12-diazaheptadecan-8-yl)amino)-6-oxohexyl)-1,1-dimethyl-2-((1E,3E,5E)-5-(1,1,3-trimethyl-6,8-disulfonato-1,3-dihydro-2H-benzo[e]indol-2-ylidene)penta-1,3-dien-1-yl)-1H-benzo[e]indol-3-ium-6,8-disulfonate (10)

8.1) Compound **9** (0.0855 g, 0.0897 mmol) and Et_3N (0.05 g, 0.538 mmol) were dissolved in DMSO (0.7 mL).

8.2) The mixture was stirred at room temperature for 15 min, and SCy5.5 (0.02 g, 0.0179 mmol) was added to reaction mixture.

8.3) After being stirred for overnight at room temperature under the dark condition, the crude mixture was purified by MPLC using methanol gradient in water to yield compound **10**.

9. *In vivo* and *ex vivo* fluorescence imaging

9.1) A FOBI Imaging System was used to perform *in vivo* fluorescence imaging and *ex vivo* biodistribution studies (NeoScience, Republic of Korea).

9.2) PBS was used to dilute the stock aqueous solution of dimeric TSPO ligand in ethanol.

9.3) C6 glioma tumor-bearing mice were injected intravenously with 20 nmol of ligand, and imaging was acquired after 6 hours.

9.4) The anesthetic mice were sacrificed by cervical dislocation after 6 hours of imaging. The organs were then gathered and placed in a plastic Petri dish (tumor, heart, liver, stomach, spleen, liver, lung, and kidneys).

9.5) Using organs of glioma mice model, *ex vivo* imaging, and fluorescence distribution calculations were obtained *via* a FOBI imaging system.

Representative Results

1. Synthesis of core TSPO structure 2

The structure of compound **2** was confirmed by ^{1}H-NMR, ^{13}C-NMR (synthesis yield from starting material: 60%). ^{1}H NMR (400 MHz, $CDCl_3$) δ 9.24 (s, 1H), 8.43 (d, J = 5.6 Hz, 1H), 8.33 (s, 1H), 7.41-7.37 (m, 2H), 7.28-7.20 (m, 2H), 6.94-6.92 (m, 1H), 6.78-6.63 (m, 5H), 4.87 (q, J = 12.4 Hz, 2H), 2.02 (s, 3H); ^{13}C NMR (100 MHz, $CDCl_3$) δ 173.6, 161.0, 156.2, 152.7, 151.2, 150.5, 131.3, 130.4 (2C), 128.0, 126.4, 121.5, 120.7 (2C), 119.4, 117.8, 110.7, 106.5, 50.3, 21.8.

2. Synthesis of linker 5

The structure of the compound **5** was confirmed by ^{1}H-NMR, ^{13}C-NMR (synthesis yield: 86%). ^{1}H H NMR (400 MHz, $CDCl_3$) δ 7.83 (d, J = 8.4 Hz, 2H), 7.38 (d, J = 8.0 Hz, 2H), 4.19-4.17 (m, 2H), 3.66-3.63 (m, 2H), 3.46 (t, J = 5.2 Hz, 2H), 3.25-3.22 (m, 2H), 2.47 (s, 3H), 1.46 (s, 9H); ^{13}C NMR (100 MHz, $CDCl_3$) δ 155.9, 144.9, 132.9, 129.8 (2C), 128.0 (2C), 79.4, 70.4, 69.1, 68.4, 60.4, 28.4 (3C), 21.7.

3. Synthesis of core TSPO structure with linker 7

The structure of the compound **7** was confirmed by ^{1}H-NMR, ^{13}C-NMR (synthesis yield: 99%). ^{1}H NMR (400 MHz, $CDCl_3$) δ 8.34 (s, 1H), 8.28 (s, 1H), 7.44-7.39 (m, 2H), 7.35 (dd, J = 7.2, 1.6 Hz, 1H), 7.29-7.25 (m, 1H), 7.23-7.19 (m, 1H), 6.88-6.83 (m, 3H), 6.77 (d, J = 8.0 Hz, 1H), 6.53 (d, J = 5.6 Hz, 1H), 5.12 (q, J = 14.0 Hz, 2H), 3.96-3.93 (m, 2H), 3.73-3.63 (m, 4H), 3.60 (t, J = 4.8 Hz, 2H), 2.96 (bs, 1H), 2.86 (bs, 1H), 2.00 (s, 3H); ^{13}C NMR (100 MHz, $CDCl_3$) δ 170.6, 160.8, 156.9, 153.2, 151.7, 150.3, 131.9, 130.3 (2C), 129.1, 128.5, 126.0, 124.8, 120.8, 120.7 (2C), 111.2, 110.3, 72.3, 69.4, 67.3, 46.3, 41.4, 22.3.

4. Synthesis of the novel dimeric fluorescent TSPO ligand 10

The structure of the compound **10** was confirmed by ^{1}H-NMR, ^{13}C-NMR (synthesis yield: 42%). ^{1}H NMR (400 MHz, CD_3OD) δ 9.12 (d, J = 9.6 Hz, 1H), 8.78 (s, 1H), 8.64 (s, 1H), 8.44 (t, J = 12.8 Hz, 1H), 8.30-8.23 (m, 5H), 8.15 (s, 1H), 7.74-7.71 (m, 1H), 7.48-7.39 (m, 5H), 7.38-7.17 (m, 11H), 6.95-6.91 (m, 6H), 6.86-6.76 (m, 4H), 6.64-6.54 (m, 3H), 6.37 (dd, J = 13.6, 4.8 Hz, 1H), 5.16-5.08 (m, 3H), 5.06-4.91 (m, 4H), 4.64 (s, 1H), 4.11 (s, 1H), 4.00-3.89 (m, 4H), 3.80-3.65 (m, 2H), 3.64-3.50 (m, 7H), 3.46-3.42 (m, 2H), 3.14-3.36 (m, 3H), 3.34-3.32 (m, 9H), 2.53-2.51 (m, 2H), 2.47-2.43 (t, J = 7.2 Hz, 2H), 2.31-2.22 (m , 2H), 2.14-2.07 (m, 2H), 2.05-1.97 (m, 6H), 1.91-1.83 (m, 2H); ^{13}C NMR (100 MHz, CD_3OD) δ 173.6, 173.3, 172.9 (2C), 172.8, 171.5 (2C), 161.4 (2C), 157.4, 157.2 (2C), 153.6, 153.0 (2C), 150.9 (2C), 150.2 (2C), 149.2, 131.4 (2C), 131.4 (2C), 130.9, 130.8, 130.2 (4C), 130.1 (2C), 129.3 (2C), 129.3 (2C), 129.7, 128.3, 128.3, 128.3, 128.2, 128.2 (2C), 127.3, 126.0 (2C), 125.6, 124.2 (2C), 124.1, 123.4, 121.9, 121.8, 120.5 (4C), 120.4 (2C), 120.3, 120.1, 111.3 (2C), 111.0, 110.6 (2C), 69.2, 69.1 (2C), 67.5, 67.3 (2C), 67.2, 56.3, 52.8, 51.3, 50.8, 46.3, 46.2 (2C), 39.2 (2C), 39.1, 37.9, 33.7, 30.9, 26.6, 26.4, 25.1, 24.9, 21.1 (2C), 16.1.

4. *In vivo* and *ex vivo* fluorescence imaging

A set of photographs collected under white and red light to visualize *in vivo* biodistribution, accumulation of a new dimeric TSPO ligand conjugated with SCy5.5 were shown in Figure 1. The distribution of

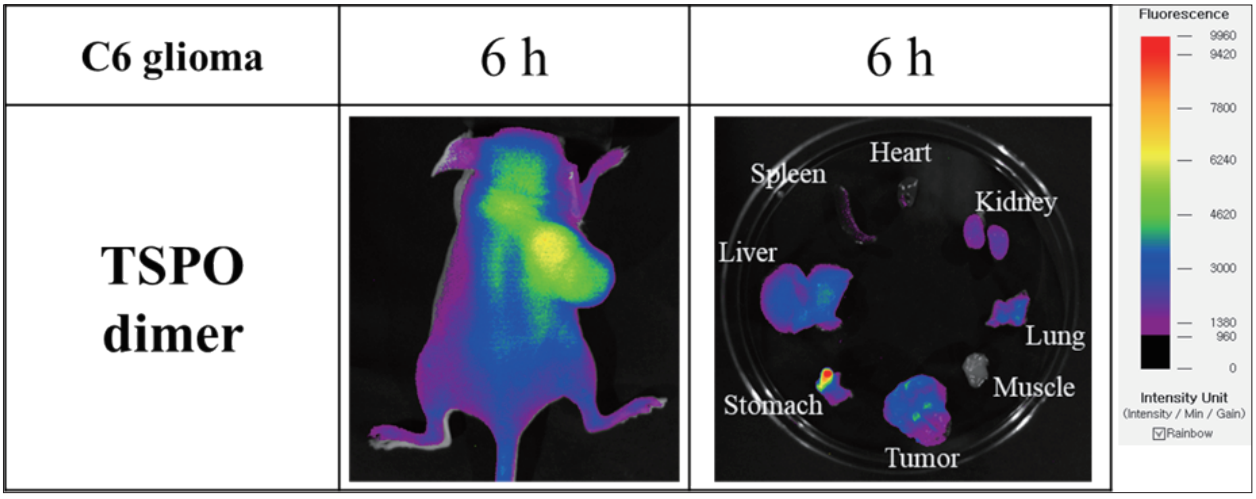

Figure 1. *In vivo* and *ex vivo* imaging study of dimeric fluorescent TSPO ligand (10) in glioma mouse model.

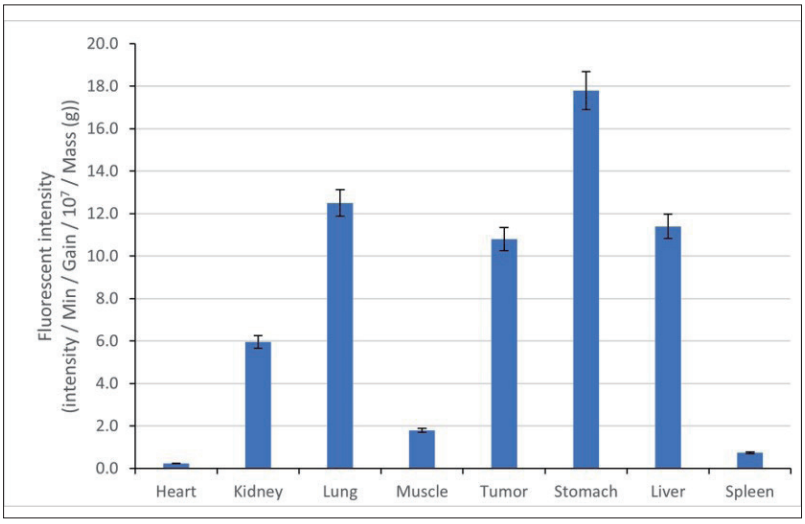

Figure 2. Biodistribution of dimeric fluorescent TSPO ligand (10) in glioma mouse model.

the chemical in all organs of the mice was observed after 1 hour of administration. The dimeric TSPO fluorescent ligand favored accumulation in the tumor region after 6 hours. For 6 hours after injection, *in vivo* and *ex vivo* tumors treated with of the mice retained the strong signal and high tumor-to-normal contrast growth. As demonstrated in Figure 2, the stomach had the maximum fluorescence intensity, followed by the lung, tumor, and liver. A little fluorescence signal was seen in the kidney and muscle. Furthermore, in the glioma mouse model injected with the new dimeric TSPO fluorescent ligand, the heart and spleen showed essentially minimal fluorescence signal.

Discussion

The synthetic procedure of PBR28-based structure has been established in the previous literature [33]. First, a four-step protocol was used to produce the *N*-(2-hydroxybenzyl)-*N*-(4-phenoxypyridin-3-yl) acetamide motif (compound **2**), beginning with 4-chloro-3-nitropyridine. The TSPO ligand was then attached to the glutamine spine through amide linkage,

followed by the conjugation of dimeric TSPO ligand with NIR probe (SCy5.5). The overall yield for synthesizing the final product (compound **10**) is 21%. Despite the ease with which PBR28-based TSPO ligands may be synthesized, the conjugation with SCy5.5 in the last step has the lowest yield of the whole procedure.

Because of the safety and popularity of the C6 glioma cell line [34], we performed TSPO *in vivo* and *ex vivo* research on xenograft mice with C6 glioma tumor to investigate the behaviors of dimeric TSPO ligand with NIR probe, SCy5.5. The mice were given 20 nmol of TSPO ligand through tail vein injection and photos were taken 6 hours later (Figure 1). After 6 hours of imaging, an *ex vivo* biodistribution research was performed, and the results indicated that the fluorescent ligands accumulated only in particular organs such as the kidneys, tumor, liver, lung, and stomach (Figure 1 and 2). Because of the modest expression of TSPO in the kidney [35], the dimeric TSPO targeting moiety can be detected in the kidney. This TSPO expression can explain the sufficient signal by ligand absorption in this organ. The fluorescence intensity signal in tumors shows that the new dimeric TSPO ligand conjugated with NIR probe may efficiently identify glioma. The increased uptake in the liver might be due to hepatobiliary excretion or non-target uptake unrelated to TSPO. Besides, the modest expression of TSPO in the lung might explain our compound's uptake signal [36].

Conclusion

In conclusion, we successfully achieved *N*-(2-hydroxybenzyl)-*N*-(4-phenoxypyridin-3-yl)acetamide based structure (PBR28 structure) (compound **2**) for targeting translocator protein (TSPO) from commercially available starting materials. Also, the novel TSPO fluorescent ligand (compound **10**) were produced *via* amide linkage with glutamine spine, and conjugated with SCy5.5, a NIR probe in 21% yield. After 6 hours of injection, *in vivo* and *ex vivo* tumor imaging of mice injected with compound **10** maintained a robust signal and a high tumor-to-normal contrast. These results proved that our compound **10** could be a promising TSPO ligand for the diagnosis of glioma.

Acknowledgements

This research was supported by the National Research Foundation of Korea (NRF) grant funded by the Korea government (MSIT) (NRF-2021R1A2C1011204).

References

1. Papadopoulos V, Baraldi M, Guilarte TR, Knudsen TB, Lacapère JJ, Lindemann P, Norenberg MD, Nutt D, Weizman A, Zhang MR, Gavish M. Translocator protein (18 kDa): new nomenclature for the peripheral-type benzodiazepine receptor based on its structure and molecular function. *Trends Pharmacol Sci* 2006;27:402–409.
2. Papadopoulos V, Liu J, Culty M. Is there a mitochondrial signaling complex facilitating cholesterol import? *Mol Cell Endocrinol* 2007;265:59–64.
3. Jorda EG, Jimenez A, Verdaguer E, Canudas AM, Folch J, Sureda FX, Camins A, Pallas M. Evidence in favour of a role for peripheral-type benzodiazepine receptor ligands in amplification of neuronal apoptosis. *Apoptosis* 2005;10:91–104.
4. Jayakumar AR, Panickar KS, Norenberg MD. Effects on free radical generation by ligands of the peripheral benzodiazepine receptor in cultured neural cells. *J Neurochem* 2002;83:1226–1234.
5. Delavoie F, Li H, Hardwick M, Robert JC, Giatzakis C, Péranzi G, Yao ZX, Maccario J, Lacapere JJ, Papadopoulos V. *In vivo* and *in vitro* peripheral-type benzodiazepine receptor polymerization: functional significance in drug ligand and cholesterol binding. *Biochemistry* 2003;42:4506–4519.
6. Lacapere JJ, Papadopoulos V. Peripheral-type

benzodiazepine receptor: structure and function of a cholesterol-binding protein in steroid and bile acid biosynthesis. *Steroids* 2003;68:569–585.
7. Chen MK, Guilarte TR. Translocator protein 18 kDa (TSPO): molecular sensor of brain injury and repair. *Pharmacol Ther* 2008;118:1–17.
8. Li F, Liu J, Zheng Y, Garavito RM, Ferguson-Miller S. Crystal structures of translocator protein (TSPO) and mutant mimic of a human polymorphism. *Science* 2015;347:555–558.
9. Maaser K, Grabowski P, Sutter AP, Höpfner M, Foss HD, Stein H, Berger G, Gavish M, Zeitz M, Scherübl H. Overexpression of the peripheral benzodiazepine receptor is a relevant prognostic factor in stage III colorectal cancer. *Clin Cancer Res* 2002;8:3205–3209 (2002).
10. Veenman L, Levin E, Weisinger G, Leschiner S, Spanier I, Snyder SH, Weizman A, Gavish M. Peripheral-type benzodiazepine receptor density and *in vitro* tumorigenicity of glioma cell lines. *Biochem Pharmacol* 2004;68:689–698.
11. Scarf AM, Ittner LM, Kassiou M. The translocator protein (18 kDa): central nervous system disease and drug design. *J Med Chem* 2009;52:581–592.
12. Matarrese M, Moresco RM, Cappelli A, Anzini M, Vomero S, Simonelli P, Verza E, Magni F, Sudati F, Soloviev D, Todde S, Carpinelli A, Kienle MG, Fazio F. Labeling and evaluation of *N*-[^{11}C]methylatedquinoline-2-carboxamides as potential radioligands for visualization of peripheral benzodiazepine receptors. *J Med Chem* 2001;44:579–585.
13. Camsonne R, Moulin MA, Crouzel C, Syrota A, Maziere M, Comar D. Carbon 11 labelling of PK11195 and visualization of benzodiazepine peripheral receptors using positron emission tomography. *J Pharmacol* 1986;17:383.
14. Taliani S, Da Settimo F, Da Pozzo E, Chelli B, Martini C. Translocator protein ligands as promising therapeutic tools for anxiety disorders. *Curr Med Chem* 2009;16:3359–3380.
15. Trapani A, Palazzo C, de Candia M, Lasorsa FM, Trapani G. Targeting of the translocator protein 18 kDa (TSPO): a valuable approach for nuclear and optical imaging of activated microglia. *Bioconjugate Chem* 2013;24:1415–1428.
16. Denora N, Laquintana V, Trapani A, Suzuki H, Sawada M, Trapani G. New fluorescent probes targeting the mitochondrial-located translocator protein 18 kDa (TSPO) as activated microglia imaging agents. *Pharm Res* 2011;28:2820–2832.
17. Manning HC, Merchant NB, Foutch AC, Virostko JM, Wyatt SK, Shah C, McKinley ET, Xie J, Mutic NJ, Washington MK, LaFleur B, Tantawy MN, Peterson TE, Ansari MS, Baldwin RM, Rothenberg ML, Bornhop DJ, Gore JC, Coffey RJ. Molecular imaging of therapeutic response to epidermal growth factor receptor blockade in colorectal cancer. *Clin Cancer Res* 2008;14:7413–7422.
18. Manning HC, Smith SM, Sexton M, Haviland S, Bai M, Cederquist K, Stella N, Bornhop DJ. A peripheral benzodiazepine receptor targeted agent for *in vitro* imaging and screening. *Bioconjugate Chem* 2006;17:735–740.
19. Escobedo JO, Rusin O, Lim S, Strongin RM. NIR dyes for bioimaging applications. *Curr Opin Chem Biol* 2010;14:64−70.
20. Kiyose K, Kojima H, Nagano T. Functional Near Infrared Fluorescent Probes. *Asian J Chem* 2008;3:506−515.
21. Hilderbrand SA, Weissleder R. Near-infrared fluorescence: application to *in vivo* molecular imaging. *Curr Opin Chem Biol* 2010;14:71–79.
22. Wang S, Li B, Zhang F. Molecular Fluorophores for Deep-Tissue Bioimaging. *ACS Cent Sci* 2020;6:1302–1316.
23. Pansare VJ, Hejazi S, Faenza WJ, Prud'homme RK. Review of long-wavelength optical and NIR imaging materials: contrast agents, fluorophores, and multifunctional nano carriers. *Chem Mater* 2012;24:812–827.
24. East AK, Lucero MY, Chan J. New directions of activity-based sensing for *in vivo* NIR imaging. *Chem Sci* 2021;12:3393–3405.
25. Liu HW, Chen L, Xu C, Li Z, Zhang H, Zhang XB, Tan W. Recent progresses in small-molecule enzymatic fluorescent probes for cancer imaging. *Chem Soc Rev* 2018;47:7140–7180.
26. Li JB, Liu HW, Fu T, Wang R, Zhang XB, Tan W. Recent progress in small-molecule near-IR probes for bioimaging. *Trends Chem* 2019;1:224–234.
27. Louis DN, Perry A, Reifenberger G, Von Deimling A, Figarella-Branger D, Cavenee WK, Ohgaki H, Wiestler OD, Kleihues P, Ellison DW. The 2016 World Health Organization classification of tumors of the central nervous system: a summary. *Acta Neuropathol* 2016;131:803−820.
28. Dhermain FG, Hau P, Lanfermann H, Jacobs AH, van den Bent MJ. Advanced MRI and PET imaging for assessment of treatment response in patients with gliomas. *Lancet Neurol* 2010;9:906−920.
29. Kozikowski AP, Kotoula M, Ma D, Boujrad N, Tückmantel W, Papadopoulos V. Synthesis and biology of a 7-nitro-2, 1, 3-benzoxadiazol-4-yl derivative of 2-phenylindole-3-acetamide: a fluorescent probe for the peripheral-type benzodiazepine receptor. *J Med Chem* 1997;40:2435−2439.

30. Scarf AM, Kassiou M. The Translocator Protein. *J Nucl Med* 2011;52:677–680.
31. Owen DR, Gunn RN, Rabiner EA, Bennacef I, Fujita M, Kreisl WC, Innis RB, Pike VW, Reynolds R, Matthews PM, Parker CA. Mixed-affinity binding in humans with 18-kDa translocator protein ligands. *J Nucl Med* 2011;52:24–32.
32. Briard E, Zoghbi SS, Imaizumi M, Gourley JP, Shetty HU, Hong J, Cropley V, Fujita M, Innis RB, Pike VW. Synthesis and evaluation in monkey of two sensitive [^{11}C]-labeled aryloxyanilide ligands for imaging brain peripheral benzodiazepine receptors *in vivo*. *J Med Chem* 2008;51:17–30.
33. Wang M, Yoder KK, Gao M, Mock BH, Xu XM, Saykin AJ, Hutchins GD, Zheng QH. Fully automated synthesis and initial PET evaluation of [^{11}C]PBR28. *Bioorg Med Chem Lett* 2009;19:5636–5639.
34. Giakoumettis D, Kritis A, Foroglou N. C6 cell line: the gold standard in glioma research. *Hippokratia* 2000;22:105.
35. Gehlert DR, Yamamura HI, Wamsley JK. Autoradiographic localization of "peripheral-type" benzodiazepine binding sites in the rat brain, heart and kidney. *Naunyn-Schmiedeberg's Arc Pharmacol* 1985;328:454–460.
36. Awad M, Gavish M. Peripheral-type benzodiazepine receptors in human cerebral cortex, kidney, and colon. *Life Sci* 1991;49:1155–1161.